Characterization of the optical properties of a PCM glazing system

Two Strategies for Reactive Power Partitioning in a Wind Farm to Satisfy the TSO Requirements and Assessment of Distribution Line Losses

Alessandro Ciocia
Dipartimento Energia "Galileo Ferraris"
Politecnico di Torino,
Torino, Italy
alessandro.ciocia@polito.it
Gabriele Malgaroli
Dipartimento Energia "Galileo Ferraris"
Politecnico di Torino,
Torino, Italy
gabriele.malgaroli@polito.it

Maria Lara Travaglini
Dipartimento Energia "Galileo Ferraris"
Politecnico di Torino,
Torino, Italy
maria.travaglini@polito.it

Gianfranco Chicco
Dipartimento Energia "Galileo Ferraris",
Politecnico di Torino,
Torino, Italy
gianfranco.chicco@polito.it

Filippo Spertino
Dipartimento Energia "Galileo Ferraris",
Politecnico di Torino,
Torino, Italy
filippo.spertino@polito.it

Abstract——This paper investigates the effects of two strategies for partitioning the reactive power among the wind turbines of a 90 MVA wind farm located in Southern Italy. The wind farm participates in the voltage regulation service and must meet a minimum reactive power requirement set by the Italian Transmission System Operator (TSO). The first partitioning strategy tested evenly distributes the reactive power among all wind turbines. The other partitioning strategy that assigns each wind turbine 90% of its maximum reactive power capacity, starting from the closest one to the grid connection point, until the total requirement is met. Simulations are performed to evaluate the ability of the wind farm to maintain the required reactive power while keeping the voltage within ±10% of the nominal voltage and remaining inside the wind turbines' reactive power capability curves. The performance of both strategies is compared in terms of meeting the TSO's reactive power requirements, voltage limitations, and Joule losses in the distribution network. The results indicate that the even distribution strategy has lower Joule losses while keeping the voltage ranges, making it the most effective approach. In contrast, the second strategy, although fulfilling the reactive power requirement, results in slightly higher energy losses. Therefore, the even partitioning strategy offers better balance of performance, simplicity, and efficiency for managing reactive power in the wind farm.

Keywords— Wind power systems, Power Flow, Grid Connection, Reactive Power Management

I. INTRODUCTION

In 2021, the Italian Transmission System Operator (TSO) promoted the contribution of large renewable power plants for voltage regulation in the High Voltage (HV) grid [1]. Voltage regulation based on reactive power support is one of the main services included in the grid codes [2][3]. Renewable power plants can contribute to reactive power support together with reactive power compensation devices like synchronous compensators, capacitor banks and static var compensators [4]. Some viable contributions to reactive power support can also be given by wind power plants, mainly depending on the location of the wind turbines in the network [5]. The purpose of the present work is to compare two strategies of reactive power partitioning among the wind turbines of a wind farm located in Southern Italy, with a nominal power of 90 MVA. Each strategy is tested through simulations and must allow the plant to continuously provide a minimum of 17.5 Mvar (capacitive or inductive) in every working condition, with the simultaneous fulfilment of the capability curve of the wind turbines and the node voltage variations falling inside the limits ±0.1 V_n, where V_n is the nominal voltage. The strategies are then compared in terms of effectiveness and efficiency, through the check of the constraints and the calculation of the Joule losses in the distribution lines that connect the wind generators each other and to the grid.

In the present work, the wind turbines are equipped with induction (asynchronous) generators and full-load frequency converters, connected to Low Voltage (LV)/Medium Voltage (MV) transformers; their capability curve, which expresses the operational limits on the active power – reactive power plane, is based on data provided by the manufacturer of the wind turbines.

The sign convention adopted is the following: positive injected reactive power (as a capacitor) and negative absorbed reactive power (as an inductor). According to the voltage regulation, when the voltage is lower than its nominal value, the wind farm behaves like a capacitor, which increases the node voltage until the nominal value is restored; conversely, when the voltage exceeds its nominal value, the system behaves like an inductor, decreasing the node voltage until the nominal value. The maximum (capacitive) and minimum (inductive) limits of reactive power that a wind turbine can inject/absorb are a function of active power generation and node voltage.

Active and reactive power monitoring data (1-minute time step) were analysed for 2 years of operation for all 39 turbines of the wind farm; the statistical analysis of the monitoring data showed that the maximum variation of reactive power was ≈ 0.12 Mvar/min for each wind turbine, i.e., 5%/min with respect to the rated active power. This technical limit was observed in a situation of normal operation of wind turbines, in which no reactive power exchange was requested by the TSO. Nevertheless, in this work, the wind farm is supposed to provide continuously reactive power to the external grid, regardless of the operating conditions of the wind farm itself. Therefore, in this stressful condition for the wind turbines, results show that higher power deviations occur to fulfil the new reactive power requirements.

II. Layout of the Wind Farm Grid Connection

The 90 MW wind farm under study is composed of 39 turbines and has a radial structure with a single connection point to the grid, as shown in Fig. 1. In the scheme, the nodes are numbered from 0 (Point of Common Coupling, PCC) to 45. The lines connecting the nodes are identified by the letter L and numbered following the node numeration. The first line (L1) represents the HV/MV transformer and node 1 is selected as the slack node.

The plant is connected to the HV grid through a 120 MVA, 150/30 kV three-phase HV/MV transformer. The power cables used in the plant are MV aluminium power cables, buried and with a trefoil pose. Cables are oversized; in fact, the wind turbine connection line to the slack node with the highest impedance is almost 20 km long and has an impedance of 2.3 Ω. The cables are modelled through the lumped parameter π model. The accuracy of the model was verified by comparison with the exact distributed parameters model of the line and the maximum deviation found was always lower than 1%.

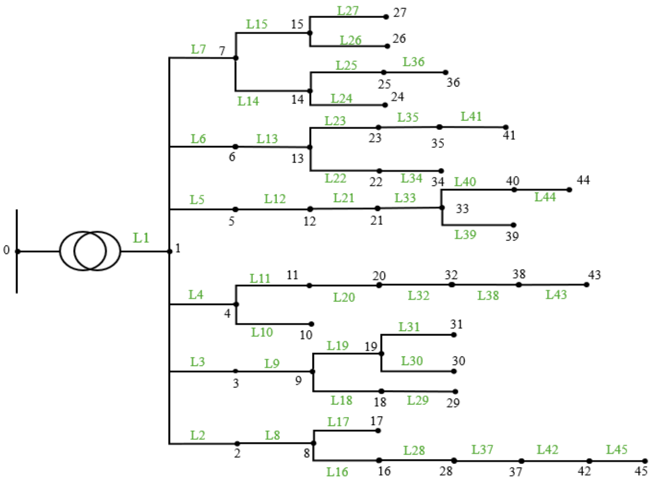

Fig. 1. Wind farm HV grid connection.

III. Analysis of Active and Reactive Power Monitoring

This section summarizes the results of the analysis of the monitoring data from the 39 turbines of the wind farm during 1 year of operation (2021). Data consist of minute-by-minute profiles of different monitored variables; this paper reports the results regarding active and reactive power, and voltage profiles.

A. Analysis of the Active Power Production

To study the actual wind turbine operation, the measured data were compared with the efficiency curve provided by the manufacturer. The efficiency values of a wind turbine are calculated as $\eta_{WT} = P_{el}/P_{wind}$, where P_{el} is the electric power and P_{wind} is the aerodynamic power. This latter is a function of wind speed, rotor area and air density [6].

Data with turbulence index below 10% are considered. The turbulence index is calculated for each time step as the ratio between the standard deviation of the wind speed and the mean value of the wind speed within a single timestep *i*, as shown in Eq. (1) [7]:

$$I_T = \frac{\sigma(v_{\mathrm{WT},i})}{\sum_{i=1}^{N} v_{\mathrm{WT},i}/N} \qquad (1)$$

The data measured during 2021 are analysed and averaged over 10 minutes, and the aerodynamic power is calculated by assuming the correct wind speed using the methodology presented in [8][9]. This methodology consists of a statistic procedure that corrects the wind speed data measured to obtain the real performance of the wind turbines. It was applied since the wind speed data were obtained through measurements made by anemometers located on the rear side of the wind turbines' nacelle, therefore they were lower than the real wind speed at the entrance of the rotor of the wind turbines.

The efficiency data calculated from the measurements are shown in Fig. 2 for a wind turbine, whose behaviour well represents the general condition of the wind farm. The coloured points can be compared with the efficiency curve from the datasheet (black curve). Most of the points are located below this curve; they are divided in points with low turbulence index I_T<0.08 (red points) and higher turbulence 0.08<I_T<0.01 (green points). Turbulence indexes higher than 0.01 are not considered, because in this condition, the manufacturer does not guarantee the correct operation of the wind turbines, and in some cases, the stop of the rotor is suggested. The data points located above the manufacturer's declared ideal curve, are not realistic (blue points). They are due to measurement errors or approximations deriving from the 10-minute data averaging and can be overlooked for the purpose of analysis; they represent only ≈3% of the data.

Regarding the effect of the pitch angle control, two groups of data were identified: efficiency values with pitch angle below 10° (light blue points) and those with pitch angle above 10° (purple points). The data with pitch angle lower than 10° are mostly located in two well-defined zones: around the cut-in speed and for wind speed values higher than 12 m/s (for which the wind turbine starts producing the nominal power). The pitch angle regulation is made at the cut-in speed to vary the angle from 0° and prepare the wind turbine for electricity production [10]. When the wind speed exceeds 12 m/s, the regulation is made to limit the active power output of the wind turbine by following the ideal efficiency curve. Data with pitch angle greater than 10° correspond mainly to high wind speed values, where the purpose is to drastically limit the power output of the wind turbine. In this way, the wind turbine does not exceed the mechanical limits defined by the manufacturer.

The same analysis was performed for all the 39 wind turbines, permitting the identification of the typical behaviour, and isolate the wind turbines with different operation. The operation of the wind turbine with the lowest efficiency is represented on the right-hand side of Fig. 3; in fact, the operation points are much further down from the curve of the manufacturer. On the

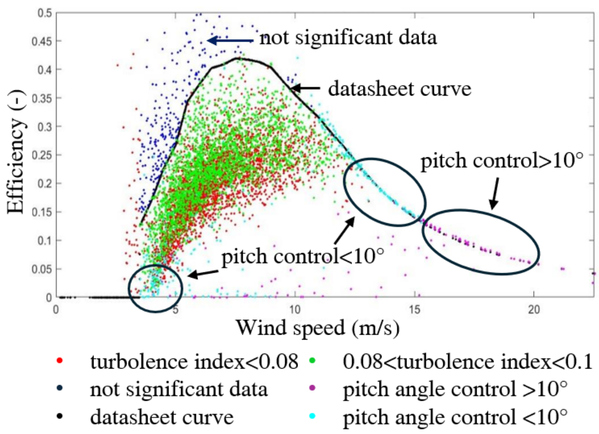

Fig. 2. Monitored active power vs. efficiency curve from the manufacturer (year 2021).

contrary, the performance of the wind turbine with the highest efficiency is represented on the left-hand side of Fig. 3; in this case, the operation points are concentrated in the highest area under the curve.

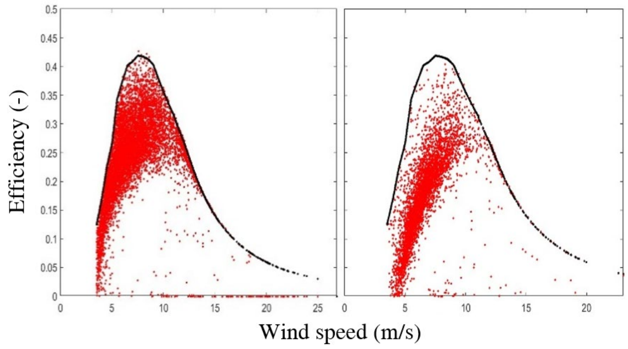

Fig. 3. Wind turbines with good performance (left) and with lower performance (right).

Table I gives the annual mean values of efficiency, power production and turbulence index of the 4 wind turbines with the lowest efficiency (first 4 rows) and of the 5 wind turbines with the highest efficiency (last 5 rows). The performance of the wind turbine with the lowest efficiency (right side of Fig. 3) is quantified in the 1st row of Table I, while the performance of the wind turbine with the highest efficiency (left side of Fig. 3) is represented in the 10th row of Table I. However, the annual average data do not highlight a correlation between efficiency and turbulence; the mean efficiency is also not directly linked to the specific power production, since the specific production depends on wind availability, which greatly varies within the wind farm area. In fact, the two furthest wind turbines are more than 10 km apart and the terrain is irregular with flat and hilly parts.

TABLE I. Specific Production for the Most and Less Efficient Wind Turbines

Mean efficiency	Specific production (kWh/year/nominal power)	Mean turbulence index
0.18	1235	0.073
0.18	1509	0.075
0.19	1268	0.076
0.19	1279	0.076
0.20	1181	0.075
0.20	1267	0.077
0.20	1535	0.074
0.20	1572	0.079
0.21	1517	0.073

B. *Analysis of the Reactive Power Exchange*

Fig. 4 shows the reactive power exchange for one day (01/01/2021) at the Point of Connection (POC) of the wind turbine connected to node 42 (refer to Fig. 1), whose behaviour well represents the whole wind farm, and the voltage trend at the POC.

The average value of reactive power is negative; i.e., the behaviour of the wind turbine is mostly capacitive.

Fig. 4 illustrates the relation between the reactive power trend and the voltage trend at the POC. The analysis reveals that during peaks in reactive power, there is a corresponding increase in voltage, ranging from 3.5% to 5.5% above the nominal value. Notably, the first peak, occurring at approximately 3:20 a.m., exceeds the nominal voltage by 5-6% for a duration of about 10 minutes. The observed voltage values remain below the Fault Ride Through (FRT) curves, indicating that the wind turbine actively participates in the grid voltage regulation.

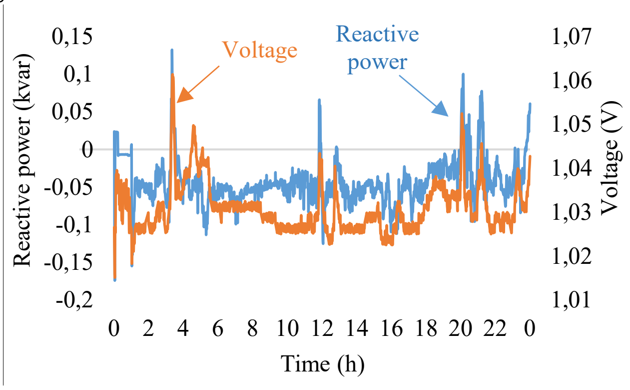

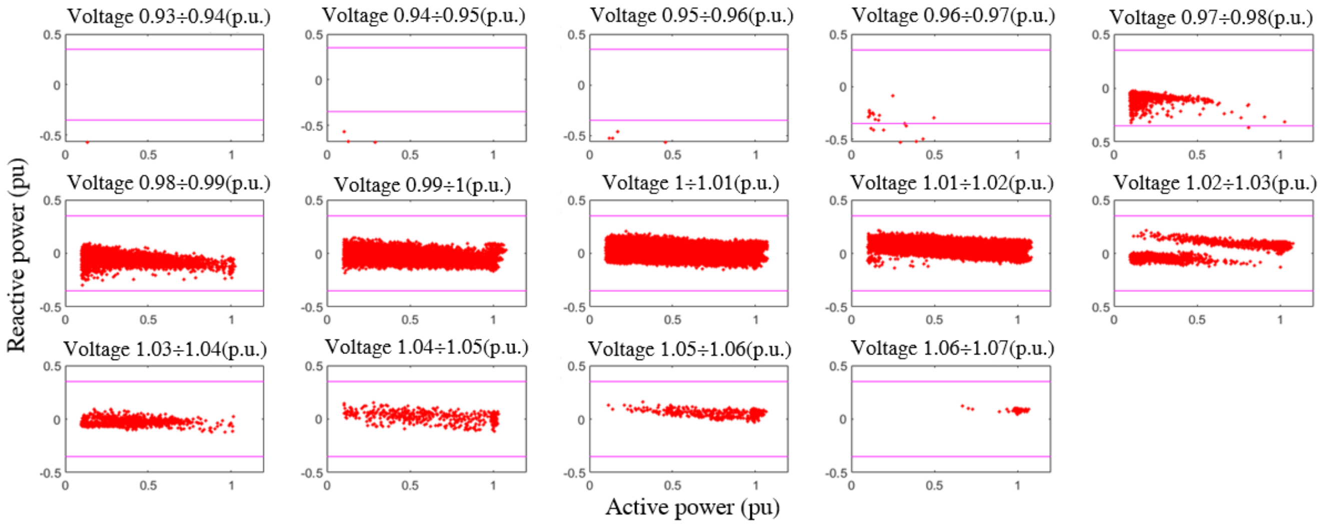

Fig. 5. P-Q diagrams for different voltage ranges.

Fig. 4. Example of reactive power and voltage profile at the POC of a wind turbine - 01/01/2021.

This is consistent with regulatory requirements, which prohibit the disconnection of the wind turbine from the grid under such conditions. In the scenario depicted in Fig. 4, the wind turbine's control system adjusted the reactive power output by increasing the delivered value, likely in response to a voltage drop on the grid, thereby maintaining the voltage inside the prescribed range.

The reactive power analysis begins with the exclusion of data corresponding to active power values that are lower than the 10% of the wind turbine’s nominal active power (2.3 MW). Data below this threshold are deemed unreliable, as per the TSO regulations, which stipulate that the active power must be sufficient to ensure a minimum performance level of the wind turbine. Additionally, data entries marked as NaN (Not a Number) are disregarded in the analysis.

Fig. 5 shows the wind turbine's P-Q planes as a function of different voltage ranges, on the basis of the monitoring data acquired (the wind turbine is connected to node 42, Fig.2). As previously mentioned, data corresponding to active power values below 10% of the nominal rating are excluded from the analysis. The TSO regulations also require that the wind turbine must be capable of providing a minimum reactive power equal to 35% of its rated active power. These limits on reactive power are inserted in the charts in Fig. 5 as a reference for the wind turbine's correct operation (purple straight lines). The results confirm that the wind turbine operates within the prescribed limits of the TSO for active-reactive power regulation, with reactive power values always within the allowable range. The wind turbine mainly regulates reactive power within voltage values ranging from 0.96 to 1.07 p.u. of the rated voltage. Outside the range 0.96÷1.07 p.u., the wind turbine does not exhibit any operational points.

IV. Power Flow Calculations by Backward Forward Sweep

The steady-state solution of a radial electrical system with a single connection point to the grid can be calculated through the Power Flow (PF) equations by an iterative calculation procedure that exploits the radial structure of the system. Knowing the system structure, loads and generations, and the voltage magnitude at the slack node, the branch currents and node voltage profiles are calculated.

One of the most used power flow methods for radial networks is the Backward Forward Sweep (BFS) [11], which exhibits excellent convergence characteristics [12] and for which some variants have been developed [13]. In the BFS, each iteration involves two computational processes: the backward and the forward sweep. During the backward process, all the currents flowing along the branches are calculated, starting from the branch of the end node towards the branch connected to the reference node (slack node). At the first iteration, the backward sweep is carried out assuming the node voltages constant at the rated voltage. In the forward sweep, the node voltages are calculated starting from the reference node to the end nodes, using the currents calculated before. The iterative process is repeated until the convergence of the algorithm is obtained. The convergence is verified by calculating the relative variation between the initial and final voltages at each node during the iteration. The iterative process ends when the relative variation is lower than a fixed tolerance.

V. Reactive Power Management Strategies

Simulations were run to compare two strategies of reactive power partitioning among the wind turbines of the plant. The strategies must ensure that the plant can satisfy the previously defined requirement of reactive power, fulfilling the voltage limits and the capability curve of the wind turbines. Then the strategies are compared through the estimation of the Joule losses.

The two selected strategies refer to different rationales. In the first case, the target is the uniform reactive power partitioning among the wind turbines, allowing for operation in relatively similar conditions and enabling prompt reactive power compensation in case one wind turbine becomes unavailable. This strategy is justified if the line impedances in the wind system are relatively small, easily allowing reactive power delivery. The other strategy aims to provide reactive power mainly from the wind turbines electrically closer to the grid connection point, also reducing the internal losses. The best performance of this strategy is expected in case of high line impedances.

A. Reactive Power Partitioning Strategy #1

The first proposed strategy shares in an even way the target reactive power (17.5 Mvar) among all the operating wind turbines of the plant. Fig. 6 shows the steps of the strategy. Each simulation starts with the import of the active power generation profiles of year 2021, line and transformer parameters, and the admittance matrix of the plant.

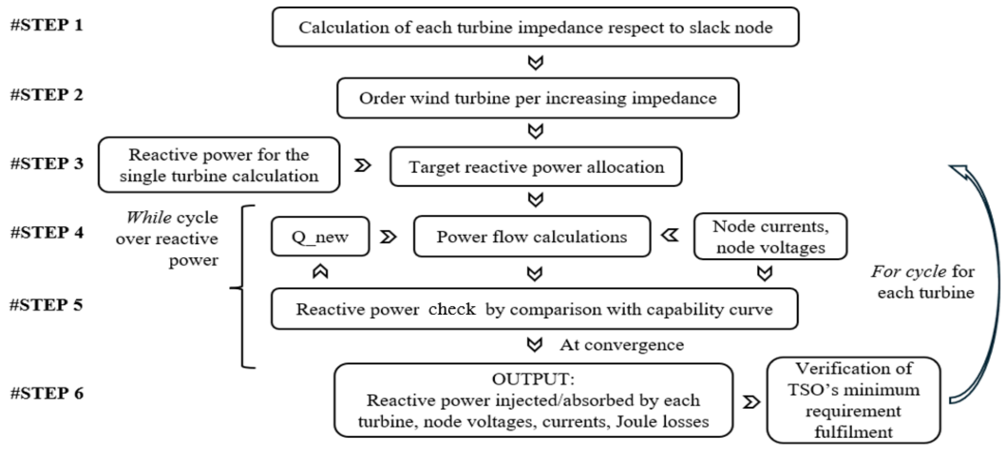

Fig. 6. Flowchart of the partitioning strategy #1.

Then, the wind turbines are ordered by increasing impedance of the wind turbine connection to the slack node (#STEP1, #STEP2); the impedance of each wind turbine connection to the slack node is calculated by summing up the impedances of all the lines that connect that wind turbine to the slack node. From the #STEP3 wind turbines are considered one-by-one; the first considered is the one with lower impedance with respect to the connection to the slack node and a reactive power value, previously calculated, is assigned to it. In this first strategy 472 kvar are assigned to each wind turbine (total: 17.5 Mvar). Power flow calculations are then performed (#STEP4), giving as output node voltages, node currents and line currents. The outcome of the BFS calculation must be verified to remain inside the capability curve of the wind turbine and satisfy the node voltage limits. The check of reactive power limits is performed through a comparison with the capability curve of the wind turbine (#STEP5). If the capability curve is not respected, the reactive power assigned to the wind turbine is reduced to the limit values. Then, the BFS power flow calculations are carried out again. This procedure is iterated until the condition $\left|\frac{Q_i^k - Q_i^{k-1}}{Q_i^k}\right| < \varepsilon$ is satisfied, where Q_i^k and Q_i^{k-1} are the reactive power assigned to the wind turbine in node *i* respectively at the iteration *k* and *k*-1, and ε is a previously defined tolerance (e.g., 0.1%). After that, the simulated data are saved (#STEP6), the following wind turbine is considered, and the process is repeated. Once all the wind turbines received a reactive power value assigned at the same minute, the Joule losses produced are calculated, and it is verified that the plant has provided at least 17.5 Mvar. If not, the minute of simulation is counted as minute of non-fulfilment of the requirement. At the end of every simulation, the voltage profiles along the branches and the node voltages are analysed, particularly in the most critical minutes, i.e., during peaks of active power generation. The extreme voltage variations at the nodes are found and verified to fall within the limits of ±0.1 V_n.

B. Reactive Power Partitioning Strategy #2

The second strategy requires each wind turbine to provide 90% of its maximum available reactive power, according to its capability curve, until the total reactive power provided/absorbed by the wind farm satisfies the minimum requirement of 18 Mvar. After calculating 90% of the reactive power capability of a wind turbine, the same steps of the previous strategy are followed, namely BFS power flow calculations are performed in a loop until the difference between the reactive power assigned to a wind turbine in two successive iterations is lower than the threshold ε. The first wind turbine is the one closest to the slack node, and this procedure is repeated for the next wind turbines in the same minute of simulation, until the total minimum reactive power injected/absorbed is reached; then, the reactive power assigned to all the remaining wind turbines is set to zero.

VI. Simulation Results

Fig. 7 shows the most relevant profiles obtained applying the first partitioning strategy. The active power and reactive power profiles (top figure), and voltage profile (bottom figure) of the wind turbine connected to node 43 (refer to Fig. 1), that is the end node of its line, are represented. These profiles are obtained from one day with high wind speed variability. The active power production reaches its nominal value of 2.3 MW six times in the day and undergoes a great variability. Nevertheless, the reactive power requirement, evenly partitioned between the wind turbines, is sufficiently small to be satisfied in every case. Although it is an end node, the voltage always remains close to the nominal value: the simulated peak is ≈1.02 p.u. This profile is a good representation of the behaviour of all the other turbines and demonstrates that the oversizing of the cables maintains voltage variations within a narrow interval. Fig. 8 represents the same profiles obtained applying the partitioning strategy #2. The profiles refer to the first wind turbine of a line of the plant, which is selected as it is one of those that mostly contribute to the reactive power injection.

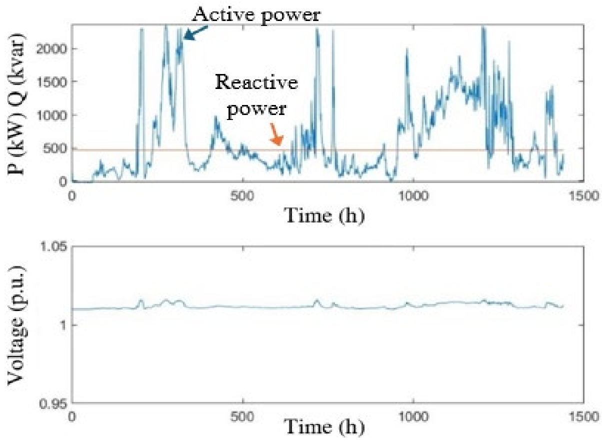

Fig. 7. Active power, reactive power and voltage profile on the end node 43 with partitioning strategy #1.

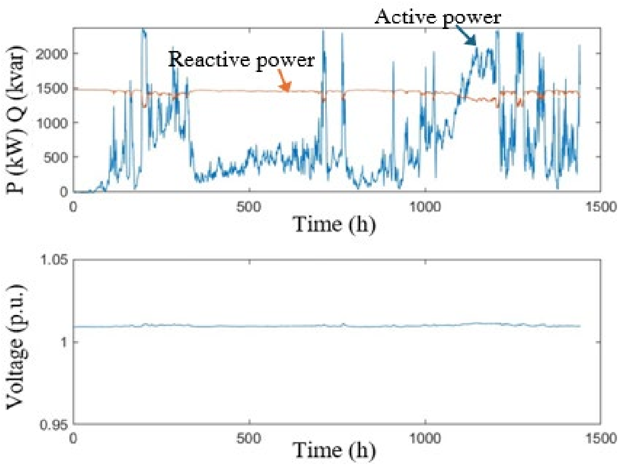

Fig. 8. Active power, reactive power and voltage profile on node 5 with partitioning strategy #2.

The reactive power injection changes according to the active power variation during the simulation, on average it injects ≈ 1450 kvar and the minimum reactive power injected is ≈ 1200 kvar around minute 200 (≈ 3 a.m.). The voltage profile is on average higher than the nominal value and the maximum is ≈ 1.01 p.u. close to midday.

Table II shows the results of the two strategies tested over a 1-year simulation; in particular, the results refer to a simulation of wind turbines continuously providing capacitive reactive power, where the voltage at the slack node is supposed always 1 p.u. The first strategy demonstrated that the plant fulfils the minimum requirement of 17.5 Mvar of the national TSO without the aid of any device for reactive power supplying, i.e. a Static Var Compensator (SVC). All the node voltages in the wind farm are always within the limits: the maximum simulated voltage is ≈1.02 p.u. thanks to the oversized cables. The limits of the capability curve of the wind turbines are always respected, and the simulated Joule losses are reduced; they are ≈0.15% of the active power yearly production. Similar results are obtained in the simulations of wind turbines continuously providing inductive reactive power. With the second strategy, the minimum requirement of 18 Mvar is also fulfilled. The node voltages always remain within limits, and the mean simulated voltage is slightly higher than the nominal one: it is on average ≈ 1.01 p.u. The estimated Joule losses are slightly higher than the previous strategy; they are ≈ 0.16% of the active power yearly production. The mean reactive power provided is a little higher than the required one: the plant provides on average ≈ 18.2 Mvar compared to the minimum (17.5 Mvar).

TABLE II. SIMULATION RESULTS OF STRATEGIES #1 AND #2 – CAPACITIVE MODE - YEAR 2021

	STRATEGY 1	STRATEGY 2
Active energy (GWh)	140	140
Reactive energy (Gvarh)	153	160
Mean node voltage (pu)	1.099	1.010

Max node voltage (pu)	1.018	1.019
Min node voltage (pu)	1.006	1.007
Joule losses (MWh)	215	223
Joule losses (%)	0.15%	0.16%
Mean reactive power (Mvar)	17.5	18.2
Reactive power required (kvar)	17.5	17.5

VII. Conclusions

The first goal of the present work has been to analyse the operation of the wind turbines of a wind farm situated in Southern Italy, in terms of active power production, efficiency and reactive power exchange. Measurements with 1-min timestep over 1 entire year were used to compare the wind turbines; the typical operation was defined permitting the identification of anomalies or low efficiencies for further analysis. This procedure was repeated for both the analysis of active and reactive power profiles. After this analysis, this paper has presented two strategies of reactive power partitioning among the turbines of the wind farm. For this purpose, the wind farm is firstly modelled in all its components; then the strategies have been tested through steady-state minute-by-minute power flow simulations. The first strategy involves even partition of the minimum reactive power among the turbines of the wind farm; the second strategy requires 90% of the maximum reactive power availability of each wind turbine until the total reactive power exchanged reaches the required target. The first strategy shows that the wind farm can satisfy the minimum requirements of reactive power, without voltage limits violations and with low Joule losses (0.16% of the production). Similar results are obtained with the second strategy, in which mainly the wind turbines closer to the PCC are requested to provide high reactive power. Voltage limits and reactive power requirements are always respected. The reason behind these similar results is due to the oversized cables connecting the wind turbines; the line impedances are remarkably low, so that in the system analysed a more sophisticated logic for reactive power partitioning does not provide significative improvements.

References

[1] Terna S.p.A., *Progetto Pilota per la Regolazione della Tensione* (in Italian), *Terna - Rete Elettrica Nazionale*, [Online]. Available: https://www.terna.it/it/sistema-elettrico/progetti-pilota-delibera-arera-300-2017-reel/progetto-pilota-regolazione-tensione. Accessed: Mar. 5, 2025].

[2] M. Mohseni and S. M. Islam, “Comparing technical connection requirements for large wind power plants,” in *IEEE Power and Energy Society General Meeting*, Detroit, MI, USA, pp. 1-8, 2011.

[3] Autorità di Regolazione per Energia Reti e Ambiente (ARERA*), Approvazione del regolamento, predisposto da Terna S.p.A., ai sensi della deliberazione dell’Autorità 300/2017/R/eel, relativo al progetto pilota per l’adeguamento di impianti “esistenti” ai sensi del Regolamento (UE) 2016/631, connessi alla rete di trasmissione nazionale, affinché possano erogare il servizio di regolazione di tensione* (in Italian), 2021. [Online]. Available: https://www.arera.it/it/docs/21/321-21.htm. [Access.: Mar. 5, 2025].

[4] R. P. Jiménez, C. A. Platero, M. E. Sánchez, and E. R. Barneto, “Synchronous Condenser for European Grid Code Compliance: A Case Study of a PV Power Plant in Spain,” *IEEE Access*, vol. 11, pp. 54713-54723, 2023.

[5] H. Li, Y. Lei, Y. Geng, H. He, Q. Niu, K. Wang, and Y. Wu, “A test methodology to verify reactive power support ability of wind turbines,” in *IEEE 5th Int. Electr. and Energy Conf. (CIEEC)*, Nangjing, China, pp. 449-454, 2022.

[6] D. Astolfi, G. Malgaroli, F. Spertino, A. Amato, A. Lombardi, and L. Terzi, “Long Term Wind Turbine Performance Analysis Through SCADA Data: A Case Study,” in *IEEE 6th Int. Forum on Res. and Tech. for Society and Industry (RTSI)*, Naples, Italy, 2021, pp. 7-12.

[7] T. Ma, H. Yang, and L. Lu, “Feasibility study and economic analysis of pumped hydro storage and battery storage for a renewable energy powered island,” *Renew. Sustain. Energy Rev.*, vol. 12, no. 9, pp. 2347–2355, Dec. 2011.

[8] F. Spertino, P. Di Leo, I.S. Ilie, and G. Chicco, “DFIG equivalent circuit and mismatch assessment between manufacturer and experimental power-wind speed curves,” *Renew. Energy*, vol. 48, pp. 333–343, Dec. 2012.

[9] J. Dai, H. Zeng, F. Zhang, H. Chen, and M. Li, “Study on Obtaining Real Power Curve of Wind Turbines Using SCADA Data,” *Front. Energy Res.*, vol. 10, Jul. 2022.

[10] A. O. Prakash, R. N. Banu, and D. Devaraj, “Maximum Energy Extraction of a Wind Farm Using Pitch Angle Control,” in *IEEE Int. Conf. on Intelligent Techniques in Control, Optimization and Signal Processing, INCOS 2019*, Apr. 2019. doi: 10.1109/INCOS45849.2019.8951361.

[11] D. Shirmohammadi, H.W. Hong, A. Semlyen, and G.X. Luo, “A compensation-based power flow method for weakly meshed distribution and transmission networks,” *IEEE Trans. Power Syst*., vol. 3, no. 2, pp. 753-762, 1988.

[12] E. Bompard, E. Carpaneto, G. Chicco, and R. Napoli, “Convergence of the backward/forward sweep method for the load-flow analysis of radial distribution systems,” *Int. J. Electr. Power & Energy Syst.*, vol. 22, no.7, pp. 521-530, 2000.

[13] U. Eminoglu and M.H. Hocaoglu, “Distribution systems forward/backward sweep-based power flow algorithms: a review and comparison study,” *Electr. Power Compon. Syst.*, vol. 37, no. 1, pp. 91–110, 2008.